JOURNAL OF SOLID STATE CHEMISTRY 69, 171–178 (1987)

BRIEF COMMUNICATION

Structure and Luminescence of Some $CsLnW_2O_8$ Compounds

C. C. TORARDI, C. PAGE, AND L. H. BRIXNER

E.I. du Pont de Nemours and Company, Central Research and Development Department and Photosystems and Electronic Products Department, Experimental Station, Wilmington, Delaware 19898*

AND G. BLASSE AND G. J. DIRKSEN

Physical Laboratory, State University, P.O. Box 80.000, 3508 TA Utrecht, The Netherlands

Received April 7, 1986; in revised form October 30, 1986

The structure of $CsLuW_2O_8$ was determined from single-crystal X-ray diffraction data with a = 9.322(3), b = 5.132(6), c = 7.277(4) Å, and β = 95.66(4)°, in the space group $P2/c$. It is composed of double chains of distorted WO_6 octahedra that share an edge across the chain and share opposite corners along the chain in the c direction. The tungsten–oxygen chains are interconnected via the lutetium and cesium atoms which are in eight- and twelve-coordination with oxygen. A comparison with the related structure of KYW_2O_8 is made. The compounds $CsLnW_2O_8$ (Ln = Y, Gd) have a similar structure. The three tungstates (Ln = Y, Gd, Lu) exhibit an intense luminescence at room temperature, whereas KYW_2O_8 does not luminesce at all. The luminescence of the compounds with Ln = Eu, Tb are also reported.

Introduction

Various structural modifications of the $CsLnW_2O_8$ compounds (Ln = La to Lu) have been reported by Trunov and Rybakov (*1*). These authors found that reversible structural transformations occur between 350° and 410°C in all but the La composition. The Er to Lu compounds show an additional transformation between 800° and 1000°C. In the low-temperature modifications, they report $CsLaW_2O_8$ to crystallize with tetragonal symmetry and $CsPrW_2O_8$ to $CsTbW_2O_8$ to have monoclinic symmetry (the space group was determined to be $P2_1/m$ on the basis of powder X-ray diffraction data). They found the Er to Lu compounds also to have monoclinic symmetry, and assigned $P2/c$ or Pc as the space group. Because of the many structural phase transitions in these compounds, they could only obtain single crystals for $CsYbW_2O_8$. The crystal structure was not determined, however. Also there are no luminescent properties reported on these compositions.

We have prepared several of these cesium rare-earth tungstates (viz., La, Sm,

* Contribution No. 4244.

0022-4596/87 $3.00

Eu, Gd, Tb, Lu) and report here on the crystal structure of $CsLuW_2O_8$ and the Raman spectra and the luminescence of these compounds.

Experimental

Samples were prepared by heating a mixture of milled Cs_2CO_3 (Johnson Matthey, 99.9%), Ln_2O_3 (Res. Chem., 99.9%), and WO_3 (Fisher, purified) in recrystallized alumina crucibles to 900–1050°C. After firing, samples were reground and reheated to ensure homogeneity. Except for $CsSmW_2O_8$, which is pale yellow, the products are white, homogeneous powders.

We also found CsCl to be an effective flux for the preparation of single crystals of $CsLuW_2O_8$. For these experiments a powder sample of α-$CsLuW_2O_8$ was mixed with 50 wt% of CsCl and sealed in a platinum tube. The tube was held at 1100°C (which is below the reported (*1*) melting point of γ-$CsLuW_2O_8$) for 30 min and then slowly cooled at 6°C/hr to room temperature. The flux was removed by water washing. Crystals up to several millimeters in length had a needle- or lath-shaped habit.

The optical measurements were performed as described before (*2*).

Information on the single-crystal X-ray data collection and structural refinement is given in Table I.[1] The data were treated for Lorentz and polarization effects, and then averaged in 2/*m* symmetry. Heavy atom positions were found by using MULTAN (*3*), and oxygen atom positions were located from difference Fourier maps. A correction for absorption was applied using DIFABS (*4*) after a full isotropic refinement was made. Only the W, Lu, and Cs atoms were refined anisotropically. It was clear from the start of the X-ray work that the crystalline quality of $CsLuW_2O_8$ had suffered as a result of the low-temperature structural phase transition which occurs at ~500°C (*1*). This is reflected in the agreement factors, in the overall standard deviations, and in the residuals peaks present in a final difference Fourier map with values up to 3.6 e/Å^3. Refinement of the structure in the acentric space group *Pc* made no improvement in the *R*-factors. The occupation numbers for Lu and Cs were also checked by including them in a final refinement. They confirmed the full occupancy of the respective sites.

Atomic positional and thermal parameters for $CsLuW_2O_8$ are given in Table II and important interatomic distances are listed in Table III. Structural figures were drawn with the assistance of the ORTEP program (*5*).

TABLE I

SUMMARY OF CRYSTAL DATA, COLLECTION DATA, AND REFINEMENT OF THE STRUCTURE $CsLuW_2O_8$

Dimensions (mm)	0.033 × 0.067 × 0.233
Diffractometer	CAD4
Radiation	Mo$K\alpha$
Monochromator	Graphite
Crystal system	Monoclinic
Cell constants	a = 9.322(3) Å
	b = 5.132(6) Å
	c = 7.277(4) Å
	β = 95.66(4)°
Calc. density (g cm^{-3})	7.09
Scan mode	ω
2θ range	0–55°
Octants	HKL, HKL
μ (cm^{-1})	531.0
Absorption correction	DIFABS[a]
Total reflections	972
Independent reflections	431 ($I > 3\sigma$)
Space group	$P2/c$
Data/parameters	11.6
R	0.089
R_w	0.086

[a] Ref. (*4*).

[1] All crystallographic calculations were performed on a Digital Equipment Corp. VAX 11/780 computer using a system of programs developed by J. C. Calabrese.

TABLE II

POSITIONAL[a] AND THERMAL[b,c] PARAMETERS FOR THE ATOMS OF $CsLuW_2O_8$

Atom	x	y	z	B_{11}	B_{22}	B_{33}	B_{12}	B_{13}	B_{23}
W	0.1869(2)	0.5205(4)	0.9922(3)	0.57(8)	0.65(8)	0.63(8)	0.04(7)	0.08(6)	−0.04(5)
Lu	0.00	0.0282(5)	0.75	0.66(11)	0.55(10)	1.08(12)	0.00	0.13(9)	0.00
Cs	0.50	0.9081(9)	0.25	1.4(2)	1.5(2)	1.8(2)	0.00	0.3(2)	0.00
O1	0.2198(38)	0.8340(55)	0.8939(44)	0.3(4)					
O2	0.1652(54)	0.6349(76)	0.2325(58)	2.0(7)					
O3	0.3572(50)	0.3972(71)	0.0580(54)	1.4(7)					
O4	0.9541(44)	0.7329(62)	0.9687(50)	1.0(6)					

[a] Space group $P2/c$ (No. 13).
[b] $\exp[-0.25(B_{11}h^2a^{*2} \ldots + 2(B_{12}hka^*b^* \ldots))]$.
[c] Oxygen atoms are isotropic.

Results and Discussion

a. Crystallographic Data

X-ray powder diffraction data were taken with a Philips APD 3600 unit. The data for $CsLaW_2O_8$ agree with those in Ref. (1). For $CsLnW_2O_8$ (Ln = Sm, Eu, Gd, Tb) the patterns agree well with the data published (*1*) for $CsPrW_2O_8$, suggesting a monoclinic cell and $P2_1/m$ space group. A comparison of the lattice parameters of $CsPrW_2O_8$ and $CsLuW_2O_8$ suggests a close structural relationship, viz., a = 9.160, b = 7.505, c = 5.357 Å, β = 91.9° for $CsPrW_2O_8$ and a = 9.322, b = 5.132, c = 7.277 Å, β = 95.7° for $CsLuW_2O_8$. Our X-ray data for the Lu compound are close to the pattern given by Trunov and Rybakov (*1*) for γ-$CsYbW_2O_8$.

TABLE III

INTERATOMIC DISTANCES (Å) FOR $CsLuW_2O_8$

W–O1	1.80(3)		Cs–O1	3.20(3)	(×2)
W–O2	1.87(4)		Cs–O1a	3.51(3)	(×2)
W–O2a	2.04(4)		Cs–O2	3.41(3)	(×2)
W–O3	1.73(5)		Cs–O3	3.11(4)	(×2)
W–O4	1.89(4)		Cs–O3a	3.14(4)	(×2)
W–O4a	2.42(4)		Cs–O3b	3.20(4)	(×2)
Lu–O1	2.42(4)	(×2)	W–Wa	3.504(4)	
Lu–O2	2.33(4)	(×2)	W–Wb	3.645(2)	
Lu–O4	2.27(3)	(×2)			
Lu–O4a	2.39(4)	(×2)			

b. Structural Description of $CsLuW_2O_8$

The structure of $CsLuW_2O_8$ contains double chains of distorted WO_6 octahedra that share edges across the chain and share opposite corners along the chain in the c direction. A section of the unit cell viewed along the c axis is shown in Fig. 1. Lutetium and cesium atoms form chains that are oriented parallel with the tungsten–oxygen double chains. Lutetium atoms form a connection between the double chains in the b direction, whereas the cesium atoms interconnect the double chains along the a axis direction.

Figure 2 shows a section of one tungsten–oxygen double chain. Within a WO_6 unit, the average W–O bond length is 1.96

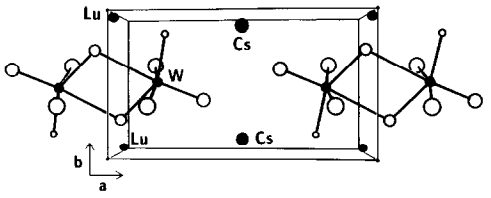

FIG. 1. A portion of the unit cell of $CsLuW_2O_8$ viewed along the c axis. The edge-shared pairs of distorted WO_6 octahedra, which are segments of the double chains running along the c axis, are shown. Metal atoms are shaded.

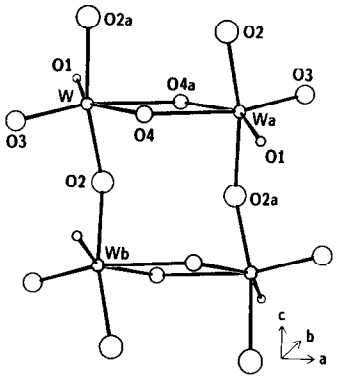

FIG. 2. A section of one tungsten–oxygen double chain in $CsLuW_2O_8$ showing the shared octahedral edges across the chain and the shared corners along the chain.

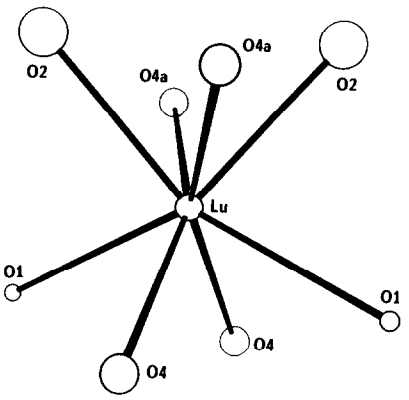

FIG. 3. The square–antiprismatic coordination around the lutetium atom in $CsLuW_2O_8$.

Å, which agrees quite well with the sum of ionic radii (*6*), 1.98 Å. Five of the six W–O bond lengths range from 1.73 to 2.04 Å but one bond, W–O4a, is very long with a value of 2.42 Å. If this weak bond were to be ignored, the tungsten atom would be surrounded by five oxygen atoms in a square pyramidal configuration. As expected, the shortest tungsten–oxygen bond length, W–O3, is trans to the long W–O bond. Related double chains composed of WO_6 octahedra are found in the compound KYW_2O_8 (*7*). However, the short and long tungsten–oxygen bond lengths occur along the chains via the corner-shared oxygen atoms in KYW_2O_8, while the long W–O bond in the present compound involves the two edge-shared oxygen atoms. This means that the bonding along the double chains is stronger for $CsLuW_2O_8$, and that the bonding across the chains (i.e., between edge-sharing pairs of WO_6 octahedra) is stronger for KYW_2O_8.

Along the double chain in $CsLuW_2O_8$, the pairs of edge-shared octahedra are alternately tipped to form a zigzag pattern in the *bc* plane. This gives rise to a bent bond angle for W–O2–W of 137(2)°. The analogous W–O–W bond angle in the related compound KYW_2O_8 (*7*) is almost linear at 172°. Similar double chains of NbO_6 octahedra in α-$PrNb_3O_9$ exhibit an average Nb–O–Nb angle of 145° along the chains (*8*).

Lutetium atoms are bonded to eight oxygen atoms in a distorted square–antiprismatic arrangement (Fig. 3). The average Lu–O bond distance is 2.35 Å and compares very well with the value of 2.36 Å obtained from the sum of ionic radii (*6*). Cesium atoms are twelve-coordinated (Fig. 4), with six of the O atoms roughly located in a plane and three O atoms above and three O atoms below the plane. This atomic

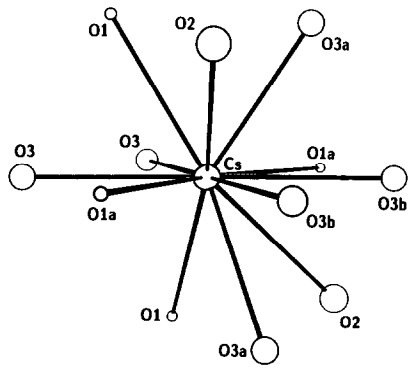

FIG. 4. The twelvefold coordination around the cesium atom in $CsLuW_2O_8$.

configuration is very similar to that found in perovskite, ABO_3, for the large A cation environment. However, the AO_{12} site is distorted in the present compound. The Cs–O bond lengths range from 3.11 to 3.51 Å with an average value of 3.26 Å to be compared with the sum of ionic radii, 3.19 Å. In KYW_2O_8, yttrium and potassium are also eight- and twelve-coordinated, respectively, with approximately the same coordination symmetry as Lu and Cs in $CsLuW_2O_8$.

The major difference between $CsLuW_2O_8$ and KYW_2O_8, in addition to the differences between the tungsten–oxygen double chains discussed above, is the manner in which the polyhedral "building blocks" are assembled. Both may be viewed as consisting of alternating "layers" oriented in the *ac* plane with one layer composed of tungsten–oxygen double chains and its adjacent layer composed of cesium–lutetium or potassium–yttrium polyhedra. However, every other W–O layer in KYW_2O_8 is shifted by $a/2$ resulting in a doubling of the b axis for this compound (*7*). Also, within the polyhedral layers of KYW_2O_8, potassium and yttrium atoms alternate along chains oriented parallel with the tungsten–oxygen double chains. In $CsLuW_2O_8$, the parallel polyhedral chains contain only cesium or only lutetium. All of the oxygen atoms are four-coordinated in both compounds.

c. Raman Spectra

The Raman spectra of $CsLnW_2O_8$ are characterized by one strong and sharp line at ~950 cm^{-1} and a line of medium intensity at ~820 cm^{-1}. These values are to be compared with, for example, 935 and ~800 cm^{-1} for $KLa(WO_4)_2$ (*9*). However, for this disordered scheelite several other peaks are observed in the spectral regions involved due to the disorder between K^+ and La^{3+} (*9*). Our results show, therefore, that the crystal structure of the compounds $CsLnW_2O_8$ does not contain a disordered sublattice. This confirms the results of the structure determination of $CsLuW_2O_8$ presented above.

Whereas the Raman spectra are very simple in the tungstate stretching frequency region, the region below 600 cm^{-1} is very complicated and characteristic of the structure type. Here we find the tungstate deformation vibrations and the lattice vibrations.

It is interesting to note that the lines observed in the tungstate stretching frequency region seem to indicate tetrahedral coordination for tungsten in contrast with the results of the structure determination. We return to this point below.

d. Luminescence

The compounds $CsGdW_2O_8$, $CsYW_2O_8$, and $CsLuW_2O_8$ show an efficient green luminescence at room temperature. $CsLaW_2O_8$ does not emit at this temperature. $CsEuW_2O_8$ shows an efficient red emission, $CsTbW_2O_8$ a green emission of medium intensity, and $CsSmW_2O_8$ no emission (300 K, ultraviolet excitation). It has been observed that the corresponding tungstates $MLnW_2O_8$ with M = Li, Na, K do not emit under these circumstances (*11*), which makes the Cs family exceptional.

First we consider the green luminescence of $CsLuW_2O_8$. Figure 5 presents some spectral data. The spectra show broad emission and excitation bands with maxima at 490 and 290 nm (7 K) and 480 and 290 nm (300 K), respectively. Between 7 and 300 K practically no temperature quenching was observed. These spectra are indicative of the tetrahedral tungstate group (*12*), especially the value of the Stokes shift. The transitions involved are of the charge-transfer type.

A weak blue emission consisting of several lines could be excited by long-wavelength ultraviolet excitation. This emission can be assigned to $^5D_3$ and $^5D_2$ emission of Eu^{3+}, which is probably present as an impu-

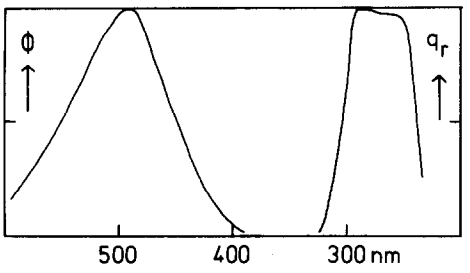

FIG. 5. The emission and excitation spectra of the luminescence of $CsLuW_2O_8$ at 7 K. Left: emission spectrum; Φ denotes the spectral power per constant wavelength interval in arbitrary units. Right: excitation spectrum; q_r denotes the relative quantum output in arbitrary units.

rity in low concentration. No $^5D_1$ or $^5D_0$ emission is observed for this excitation. Nonradiative transitions between the ^5D_J levels of Eu^{3+} have therefore only a low probability. This excludes coupling to the tungstate stretching vibrations.

The luminescence properties of $CsGdW_2O_8$ and $CsYW_2O_8$ are very similar to those of $CsLuW_2O_8$. There is no temperature quenching up to 300 K. The maximum of the emission band is at 500 (7 K) and 490 nm (300 K). The corresponding excitation bands peak at 315 and 310 nm, respectively. On the other hand, the luminescence of $CsLaW_2O_8$ is quenched at room temperature.

It is interesting to note that the spectral data point to tetrahedral coordination for tungsten, whereas the structure determination shows clearly that this is not the case. This may serve as a warning if one uses spectral data to derive the tungsten coordination in tungstates.

However, this observation is not unique and has some precedence. In $HgWO_4$, for example, vibrational as well as electronic spectra point to tetrahedral coordination (*10, 13*), whereas the structure determination shows it to be octahedral (*14*). Since this octahedral cooordination consists of four oxygen neighbors at shorter and two at longer distances, it was assumed (*10, 13*) that the spectral observations were determined by the nearest oxygen neighbors only. The situation in $CsLuW_2O_8$ seems to be similar. It is clear that the only way out of such a rough approximation is a calculation of the energy level structure of the tungstate double chain in $CsLuW_2O_8$. This formidable task lies clearly outside the present investigation.

It is striking that KYW_2O_8 does not luminesce whereas the cesium compounds do. The structural differences in the double chains of tungstate octahedra are not large. However, in KYW_2O_8 it also is possible to distinguish four O^{2-} ions which are clearly at shorter distances than the remaining two. A possible reason for the absence of luminescence in KYW_2O_8 is delocalization of electronic charge in the tungstate double chain. In this way we explained the difference in luminescence of the α and β modification of $LaNb_3O_9$ (*2*). The larger W–O–W angle in KYW_2O_8 mentioned above might be an indication in this direction.

Let us now turn to $CsEuW_2O_8$. In spite of the high Eu^{3+} concentration the Eu^{3+} emission is very efficient and the role of concentration quenching is only small. Under whatever excitation wavelength, the emission consists of Eu^{3+} emission only. The excitation spectrum of the Eu^{3+} emission consists of the characteristic Eu^{3+} lines and a band corresponding with the tungstate absorption band. These observations are made at all temperatures. Therefore, we have to conclude that excitation in the tungstate group is followed by efficient energy transfer to the Eu^{3+} ions. Since every tungstate group will have a number of nearest Eu^{3+} neighbors, this efficient transfer is to be expected and should be temperature independent (*15*).

The Eu^{3+} emission contains only the $^5D_0 \rightarrow {}^7F_J$ transitions, whatever the excitation. The higher-level emissions are obviously quenched by cross-relaxation. The spec-

trum is given in Fig. 6. The $^5D_0$–$^7F_0$ transition is extremely weak, the $^5D_0$–$^7F_1$ transition contains two lines, and the $^5D_0$–$^7F_2$ contains three lines. This suggests one crystallographic site for Eu^{3+}. It is, once again, clear that the crystal structure is completely ordered. The site symmetry which accounts most satisfactorily for this emission spectrum is S_4. It yields: 0–0 zero, 0–1 two, and 0–2 three lines. Since the 0–0 intensity is not completely zero, S_4 can only be an approximate site symmetry. It is interesting to note that these results agree with the structure of $CsLuW_2O_8$, which is further evidence that these structures are related.

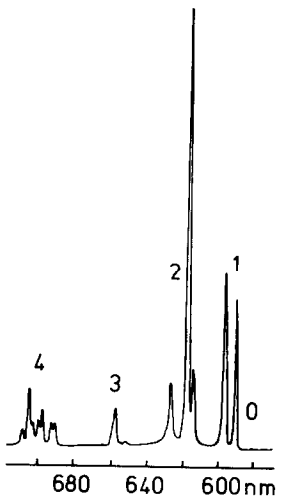

FIG. 6. The emission spectrum of $CsEuW_2O_8$ at 7 K. Excitation wavelength 310 nm. The figures denote the value of J in the transitions $^5D_0$–^7F_J.

Concentration quenching of the Eu^{3+} emission occurs by energy migration within the Eu^{3+} sublattice to quenching sites (*16*). Our results indicate that the migration probability is relatively low for the case of $CsEuW_2O_8$. For low temperatures, this is obvious in view of the forbidden character of the $^5D_0$–$^7F_0$ emission and absorption transitions (*16*). At higher temperatures thermal activation of the $^7F_1$ level may lead to migration. However, if the compound is pure, this does not necessarily lead to quenching, as has been observed for $EuAl_3B_4O_{12}$ (*17*). In $EuAl_3B_4O_{12}$ the shortest Eu–Eu distances are about 6.0 Å. Using the crystallographic data of $CsLuW_2O_8$, the shortest Eu–Eu distance in $CsEuW_2O_8$ is even longer, viz., 6.2 Å. Although this value may be incorrect, it illustrates that it is unlikely that the Eu^{3+} ions in $CsEuW_2O_8$ are on a sublattice with short internuclear distances.

The emission spectrum of $CsTbW_2O_8$ shows the well-known $^5D_4$–^7F_J transitions of the Tb^{3+} ion. The emission is of medium intensity and is temperature and excitation-wavelength independent. For tungstate excitation the Tb^{3+} output is one order of magnitude lower than the Eu^{3+} output. However, no tungstate emission could be observed, not even at 4.2 K. The lower intensity is ascribed to the occurrence of quenching by electron transfer (*18, 19*). The absence of luminescence in the case of the Sm^{3+} compound is ascribed to cross-relaxation between Sm^{3+} ions (*20*).

Finally, we note that under X-ray excitation the luminescence efficiency is conerably lower than under ultraviolet excitation. The most efficient emission under X-ray excitation was observed for $CsGdW_2O_8$, for which the luminescence efficiency is only one-fourth that of $CaWO_4$.

References

1. V. K. TRUNOV AND V. K. RYBAKOV, *Russian J. Inorg. Chem.* **19,** 188 (1974).
2. H. C. G. VERHAAR, H. DONKER, G. J. DIRKSEN, M. J. J. LAMMERS, G. BLASSE, C. C. TORARDI, AND L. H. BRIXNER, *J. Solid State Chem.* **60,** 20 (1985).
3. P. MAIN, L. LESSINGER, M. M. WOOLFSON, G. GERMAIN, AND J. P. DECLERG, "MULTAN 78: A System of Computer Programs for the Automatic Solution of Crystal Structures from X-Ray Diffraction Data," York, England and Louvain-la Neuve, Belgium (1978).

4. N. WALKER AND D. STUART, *Acta Crystallogr., Sect. A* **39,** 158 (1983).
5. C. K. JOHNSON, "ORTEP: A FORTRAN Thermal-Ellipsoid Plot Program for Crystal Structure Illustration," Oak Ridge National Laboratory Report 5138, Oak Ridge, TN (1976).
6. R. D. SHANNON, *Acta Crystallogr., Sect. A* **32,** 751 (1976).
7. S. V. BORISOV AND R. F. KLEVTSOVA, *Soviet Phys. Crystallogr.* **13,** 420 (1968).
8. C. C. TORARDI, L. H. BRIXNER, AND C. M. FORIS, *J. Solid State Chem.* **58,** 204 (1985).
9. W. J. SCHIPPER AND G. BLASSE, *Z. Naturforsch., B: Anorg. Chem., Org. Chem.* **29,** 340 (1974).
10. G. BLASSE, *J. Inorg. Nucl. Chem.* **37,** 97 (1975).
11. L. H. BRIXNER, unpublished measurements; G. BLASSE AND W. J. SCHIPPER, unpublished measurements.
12. G. BLASSE, *Structure and Bonding* **42,** 1 (1980).
13. G. BLASSE AND G. P. M. VAN DEN HEUVEL, *J. Luminescence* **9,** 74 (1974).
14. W. JEITSCHKO AND A. W. SLEIGHT, *Acta Crystallogr., Sect. B* **29,** 869 (1973).
15. W. T. DRAAI AND G. BLASSE, *Phys. Status Solidi A* **21,** 569 (1974).
16. G. BLASSE, *J. Less-Common Met.* **112,** 1 (1985); *Recl. Trav. Chim. Pays-Bas* **105,** 143 (1986).
17. F. KELLENDONK AND G. BLASSE, *J. Chem. Phys.* **75,** 561 (1981).
18. G. BLASSE AND A. BRIL, *Philips Res. Rep.* **22,** 481 (1967).
19. G. BLASSE AND N. SABBATINI, *Mater. Chem. Phys.* **16,** 237 (1987).
20. See, e.g., G. BLASSE, *in* "Energy Transfer Processes in Condensed Matter" (B. DiBartolo, Ed.), p. 251, Plenum, New York (1984).